Systems/Circuits

Elevated Correlations in Neuronal Ensembles of Mouse Auditory Cortex Following Parturition

Gideon Rothschild,[1,2] **Lior Cohen,**[1,2] **Adi Mizrahi,**[1,2] **and Israel Nelken**[1,2]

[1]Department of Neurobiology, Institute of Life Sciences and [2]Edmond and Lily Safra Center for Brain Sciences, Hebrew University of Jerusalem, Jerusalem 91904, Israel

The auditory cortex is malleable by experience. Previous studies of auditory plasticity have described experience-dependent changes in response profiles of single neurons or changes in global tonotopic organization. However, experience-dependent changes in the dynamics of local neural populations have remained unexplored. In this study, we examined the influence of a dramatic yet natural experience in the life of female mice, giving birth and becoming a mother on single neurons and neuronal ensembles in the primary auditory cortex (A1). Using *in vivo* two-photon calcium imaging and electrophysiological recordings from layer 2/3 in A1 of mothers and age-matched virgin mice, we monitored changes in the responses to a set of artificial and natural sounds. Population dynamics underwent large changes as measured by pairwise and higher-order correlations, with noise correlations increasing as much as twofold in lactating mothers. Concomitantly, changes in response properties of single neurons were modest and selective. Remarkably, despite the large changes in correlations, information about stimulus identity remained essentially the same in the two groups. Our results demonstrate changes in the correlation structure of neuronal activity as a result of a natural life event.

Introduction

Experience-dependent functional plasticity at the level of single neurons has been observed in a number of cortical regions. A large number of studies have revealed a high level of functional plasticity in primary auditory cortex (A1, see review of early work) (Weinberger, 2004). For example, receptive fields of neuronal clusters have shown stimulus-dependent changes after classical conditioning (Bakin and Weinberger, 1990). Other studies have demonstrated that experience-dependent changes in single-cell response properties result in a modified tonotopic map in A1 (Recanzone et al., 1993). The initial expression of such changes may occur within minutes after experience (Fritz et al., 2003).

However, processing in the cortex involves complex interactions of large populations of neurons, and these interactions cannot be inferred from single-cell recordings. Specifically, correlation patterns within neuronal ensembles may critically affect information processing (Zohary et al., 1994b; Abbott and Dayan, 1999; Sompolinsky et al., 2001; Averbeck and Lee, 2006; Cafaro and Rieke, 2010). Thus, to fully understand experience-dependent cortical reorganization, changes in the correlation structure of neuronal ensembles must be monitored in addition to the responses of single neurons.

In this study, we investigated how the responses of local populations of neurons in A1 change after a natural and behaviorally relevant experience. We used a complex but natural change in the life of mice and other mammals: giving birth and becoming a mother. Becoming a mother, especially for the first time, involves physiological, hormonal, behavioral, and social changes (Brunton and Russell, 2008; Leuner et al., 2010). After birth, the mother learns to take care of her pups and expresses a wide range of maternal behaviors. Some of these behaviors rely heavily on auditory communication (Noirot, 1972). For example, mothers learn to identify specific calls emitted by the pups, such as ultrasonic vocalizations (USVs) and lower-frequency wriggling calls, and respond with a variety of maternal behaviors (Geissler and Ehret, 2002, 2004; Ehret, 2005). Thus, becoming a mother reflects a dramatic, naturally occurring change, which involves behaviorally guided auditory learning. Previous studies have described changes in single-neuron response properties in mothers compared with virgins (Liu et al., 2006; Liu and Schreiner, 2007; Cohen et al., 2011). However, whether and how network-level coding is changing to accommodate this plasticity remains largely unknown.

To compare the activity of neuronal ensembles in mothers and virgins, we performed *in vivo* two-photon calcium imaging in A1 of mother mice 4–5 d after birth and compared it with responses in age-matched virgin females. This method allowed us to examine changes in responses of single neurons as well as in the correlation structure of the local population. Focusing on layer 2/3, we found major changes in network dynamics, which could not be predicted from the responses of single neurons.

Received Oct. 1, 2012; revised June 26, 2013; accepted June 28, 2013.

Author contributions: G.R., A.M., and I.N. designed research; G.R. and L.C. performed research; G.R., L.C., A.M., and I.N. analyzed data; G.R., A.M., and I.N. wrote the paper.

This work was supported by a European Molecular Biology Organization Postdoctoral Long Term Fellowship to G.R., an Edmond and Lily Safra Center Postdoctoral Fellowship to G.R., a European Research Council Grant 203994 to A.M., the United States–Israel Binational Science Foundation to I.N., and the Gatsby Charitable Foundation.

The authors declare no competing financial interests.

Correspondence should be addressed to either Dr. Adi Mizrahi or Dr. Israel Nelken, Department of Neurobiology, Institute of Life Sciences, Hebrew University of Jerusalem, Jerusalem, 91904, Israel. E-mail: mizrahi.adi@mail.huji.ac.il or israel@cc.huji.ac.il.

DOI:10.1523/JNEUROSCI.4656-12.2013

 0270-6474/13/3312851-11$15.00/0

Materials and Methods

Animal preparation. We used female NMRI mice ($n = 23$, 8–10 weeks old), anesthetized using ketamine (100 mg/kg) and medetomidine (0.83 mg/kg). Virgin mice were females that were never housed with males or pups after they had been weaned at postnatal day 21. Mothers were females 4–5 d after parturition, nursing a litter of at least five pups.

Depth of anesthesia was assessed by monitoring the pinch withdrawal reflex. Dextrose–saline was injected subcutaneously to prevent dehydration. Body temperature was maintained at 36–37°C. The skull was exposed, cleaned, and dried. A metal pin was glued to the skull and attached to a custom-made head holder, allowing precise orientation of the head relative to the objective. The muscle overlying the left A1 was removed, and a craniotomy (3 mm in diameter) was performed. The dura was gently removed, and the cortical surface was kept continuously moist. After each experiment, animals were euthanized with an overdose of sodium pentobarbital. All experiments were approved by the Hebrew University Animal Care and Use Committee. Hebrew University is an Association for Assessment and Accreditation of Laboratory Animal Care-accredited institution.

Dye loading and two-photon imaging. Dye loading was performed as previously described, targeting L2/3 neurons of A1 (Rothschild et al., 2010). To target A1, we performed a craniotomy at the following coordinates: 2.3 mm posterior and 4.2 mm lateral to bregma. Within the craniotomy, imaging was performed at a location devoid of large blood vessels, to allow optimal optical access. A1 was loaded with Fluo-4 AM (F14201; Invitrogen) using multicell bolus loading (Stosiek et al., 2003). Fluo-4 AM was dissolved in 20% Pluronic F-127 in DMSO (P-6867; Invitrogen) to a concentration of 10 mM and further diluted 10-fold in external buffer containing the following (in mM): 125 NaCl, 5 KCl, 10 glucose, 10 HEPES, 2 $CaCl_2$, 2 $MgSO_4$, and 0.1 Sulforhodamine 101. Injections were performed under visual guidance using two-photon excitation. The solution was slowly injected into the cortex (duration 30–180 s) using a quartz pipette. In some experiments, several injections were made within a distance of a few hundred micrometers. The craniotomy was glass coverslipped and secured with dental cement. The mouse was placed under the microscope, and the cranial window was oriented perpendicular to the objective lens.

Imaging was performed on an Ultima microscope (Prairie Technologies) with a 40× (0.8 NA, Olympus) or a 16× (0.8 NA, Nikon) water-immersion objective. A femtosecond laser (Mai-Tai Spectra Physics) was used to excite Fluo-4 at 820 nm. Line scan images were acquired at 100–150 Hz, depending on the length of the line. Neurons were imaged at depths of 250–380 μm under the pia, corresponding to layers 2/3 of the cortex. Imaging was stable with no movements caused by heartbeat or respiration. Imaging started 30 min after injection and lasted for ~3 h. Scan timings, stimuli delivery, and electrophysiological recordings were acquired using a standard data acquisition board (Digidata 1440A, Molecular Devices) on a separate PC.

Electrophysiological recordings. Electrodes (4–7 MΩ) were pulled from filamented, thin-walled, borosilicate glass (outer diameter, 1.5 mm; inner diameter, 1.0 mm; Hilgenberg) on a vertical two-stage puller (PC-12, Narishige). Internal solution contained the following (in mM): 140 K-gluconate, 10 KCl, 10 HEPES, 10 Na_2-phosphocreatine, 4 MgATP, 0.4 Na_2GTP, 0.5 EGTA, adjusted to pH 7.25 with KOH. Electrodes were inserted into A1, attempting to target neurons at depths of 250–400 μm, to match the imaging experiments. An increase of the pipette resistance to 10–200 MΩ resulted in most cases in the appearance of spikes. The detection of a well-separated spike was the only criterion to start the auditory protocol. Electrode signals were amplified by an intracellular amplifier in current-clamp mode (Multiclamp 700B, Molecular Devices), filtered with a 50 Hz high pass filter, and sampled at 10 kHz (Digidata 1440A, Molecular Devices).

Auditory stimulation. USVs were recorded with a 1/4 inch microphone, connected to a preamplifier and an amplifier (Bruel and Kjaer), from P4-P5 pups isolated from their mother and placed in a custom-built sound-shielded box. Vocalizations were sampled at 500 kHz using a Digidata 1322A card (Molecular Devices). USVs were identified offline, and three were selected for use in the electrophysiological experiments based on their high SNR. Other auditory stimuli were generated online using custom-written software (MATLAB; MathWorks). All stimuli were transduced to analog voltage (PCI-6731 card, National Instruments), attenuated (PA5, Tucker Davis Technologies), and presented through an electrostatic loudspeaker driver and loudspeaker (ED1, ES1 Tucker Davis Technologies). The loudspeaker was placed ~10 cm from the right ear of the mouse. Acoustic stimuli consisted of pure tones at 10, 20, and 60 kHz, a synthetic wriggling call composed of pure tones at 3.8, 7.6, and 11.4 kHz (Ehret, 2005), broadband noise (BBN), and the three ultrasonic vocalizations, for a total of 8 stimuli. Each stimulus was presented 20 times per series, pseudo-randomly shuffled, at a single intensity level (70 dB SPL, as estimated by measuring sound level with a Bruel and Kjaer microphone at the location of the head of the animal). The duration of all synthetic stimuli was 100 ms, including 5 ms ON and OFF linear ramps, whereas USV duration was ~70 ms. Interstimulus interval was 700 ms.

Data analysis. All ΔF/F traces were smoothed using a finite impulse response low-pass filter with a cutoff frequency of the sampling frequency divided by 10. To keep the temporal features of the calcium signal in their correct locations, the MATLAB function filtfilt was used to achieve zero-phase filtering (MathWorks). The quality of traces was calculated based on the S/N ratio of the transients relative to the baseline fluorescence fluctuations as described previously (Rothschild et al., 2010), and traces that did not pass a quality threshold were excluded from further analysis. Response strength was quantified as the integral of the fluorescence signal within a window of 250 ms after stimulus onset. To verify that window duration did not impact our conclusions, analyses were performed using other window durations as indicated in the text.

For both imaging and electrophysiological data, to determine whether a neuron was responsive to a specific stimulus, we tested whether its responses to the 20 stimulus presentations were significantly larger than the signal preceding stimuli onset using a t test at a significance level of 0.05. For the imaging data, this consisted of comparing integrals of the fluorescence signal from 0 to 250 ms after stimuli onset to integrals from −250 to 0 ms. For electrophysiology, we compared spike counts from 0 to 100 ms to −100 to 0 ms relative to stimuli onset. This allowed us to determine to which stimuli each neuron is responsive. A neuron was considered as responsive if it was responsive to at least one of the eight stimuli. Time to response onset in the electrophysiological data was calculated in the following way. A poststimulus time histogram was created for each responsive neuron over all trials of pure tone stimuli only, as they shared the same temporal envelope. Response onset was identified as the time of first crossing of a normalized firing rate threshold using an automated procedure. The threshold was set at the mean firing rate across the PSTH window, from −100 ms to +700 ms relative to stimulus onset.

To calculate noise correlations (NCs), we subtracted the mean response of each neuron to each stimulus from all the single-trial responses of the neuron to that stimulus. This resulted in a vector of fluctuations around the mean responses to the different stimuli. The correlation coefficients between pairs of such vectors were used as estimates of the NC between the two neurons. Stimulus-dependent NCs were again correlation coefficients calculated using only trials of a single stimulus.

For higher-order correlation analyses, we grouped fluctuation vectors of all simultaneously imaged neurons into "fluctuation matrices," in which a cell in row i and column j contains the fluctuation in response of neuron i to stimulus j around its mean response to the stimulus presented in that trial. These matrices were then simplified by keeping only the sign of each fluctuation, resulting in matrices of 1's and −1's corresponding to a response being above or below the corresponding mean. Thus, for a group of N neurons, every column of such matrix corresponded to a single-trial network fluctuation pattern. We calculated the observed probability of all patterns in which a given k neuron positively fluctuated and compared it with its expected rate under a model of independent fluctuations, which is the product of the probabilities of the activated single neurons in the given pattern.

We evaluated the amount of information about the stimuli carried by the responses using a decoding approach. For each imaging session of one ensemble of neurons, decoding was performed on the single-trial response vectors, which consisted of the responses of all neurons in that trial. We observed that in a given recording location there were often

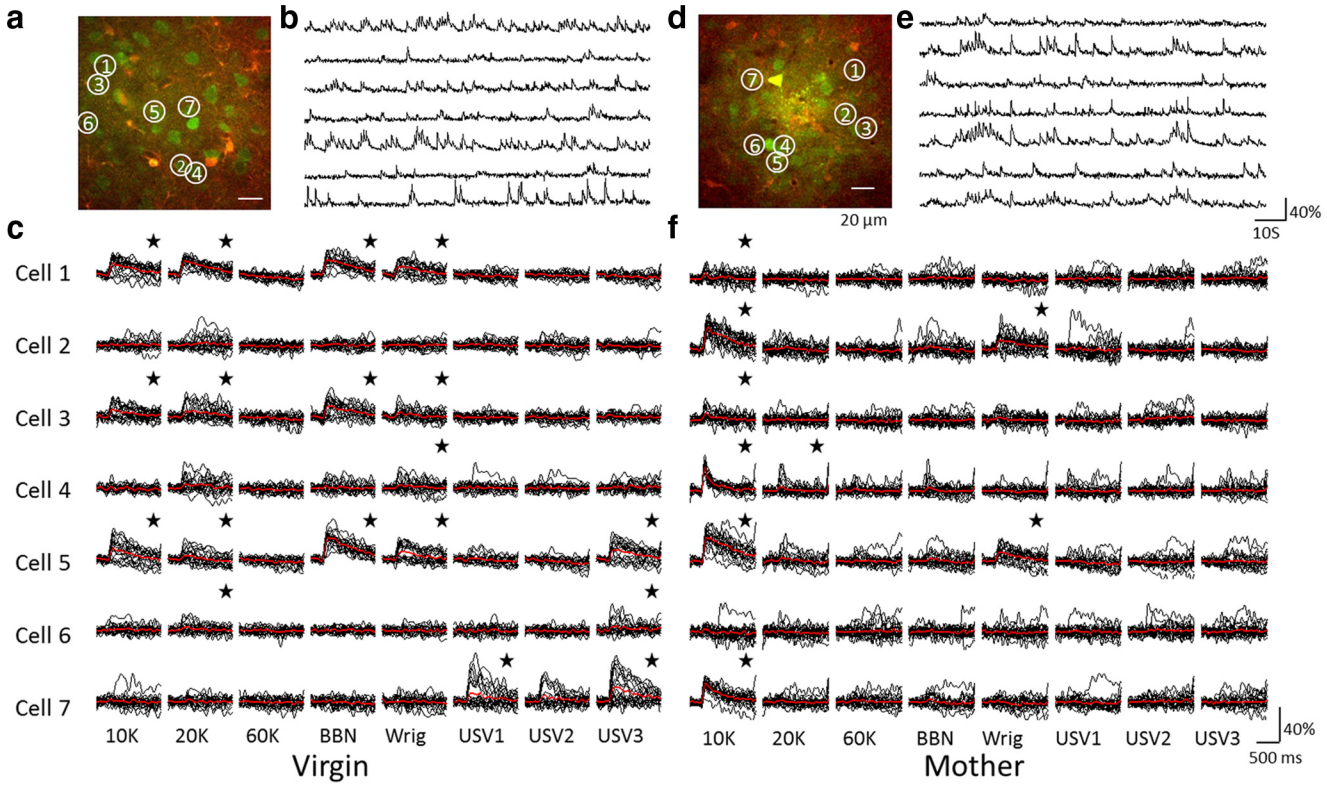

Figure 1. Imaging network responses to synthetic and natural sounds. ***a***, *In vivo* two-photon micrograph of a single optical plane in A1 of a virgin mouse after bolus loading of Fluo-4 AM (green) and SR101 (red). Some of the cells are circled and numbered. This optical plane is 362 μm below the pia. Scale bar represents 20 μm. ***b***, Relative changes in fluorescence (ΔF/F) of the seven neurons shown in ***a*** during presentation of a stimuli series (data not shown). Scale bars as in ***e***. ***c***, Single trial and mean responses of the seven neurons from ***a*** and ***b*** to eight different stimuli. Rows mark neurons 1–7 from top to bottom and columns mark different stimuli (annotated on the bottom). Each panel represents the responses to all trials of the specific stimulus (black) and its mean (red). *Panels that show a significant response. Scale bars as in ***f***. ***d–f***, Same as ***a–c***, but from a lactating mother.

stimuli to which none of the neurons responded. Decoding was therefore performed only for a subset of the eight stimuli. This subset was selected by considering all subsets of stimuli of size 4 or larger. For each such subset, we measured how well single neurons separated between the stimuli. This was done by performing a one-way ANOVA on the single trial responses to all stimuli in the subset. The figure of merit that we used to characterize the single-neuron performance was the resulting p value of the ANOVA. Then, the figure of merit for the subset consisted of the 35% percentile of the p values of all the neurons on that subset. Finally, the subset with the minimal figure of merit (because small p represents good performance) was selected for testing classification performance. Thus, the best subset of stimuli had at least one third of the neurons showing better discrimination than that shown by the best one third of the neurons on any other subset of stimuli. The stimuli that belonged to each subset were approximately equally distributed among all eight stimuli when considering all imaging sessions. All further calculations were done for that subset. The selection did not use correlations, but only single-neuron performance.

To make sure our results are not biased by the type of classifier, we initially used three types of classifiers: nearest neighbor, boosted trees, and linear discriminant classifiers implemented in the MATLAB Statistical Toolbox (MathWorks). The results obtained from these were similar, and we chose the linear discriminant analysis because it had the best classification performance.

To evaluate the performance of the classifier, we used a leave-one-out procedure. For each trial, we trained the classifier using all other trials and used the resulting classifier to classify the response to the left-out trial. We then calculated the percentage loss, defined as the rate of trials classified to a stimulus other than their own. We measured a steady bias of ~5% using this procedure, such that, for example, random data classified to four classes showed a loss of ~70% instead of 75%. This bias was uniform and small relative to the classification performance of the real data. To remove NC while maintaining single-cell response statistics, responses of each stimulus type were permuted between trials of the same stimulus independently for each neuron.

Results

To test the effect of maternity on responses of single neurons and neuronal populations in A1, we first performed *in vivo* two-photon calcium imaging in anesthetized mice while presenting both synthetic and natural sounds. We imaged two groups of mice: lactating mothers 4–5 d after parturition ($n = 6$ mice) and age-matched virgin females, as controls ($n = 9$ mice). We loaded cells in A1 with the calcium indicator Fluo-4 AM using the multicell bolus loading technique (Stosiek et al., 2003). Fluo-4 stained dozens of cells within a small sphere of ~150 μm in diameter around the injection site. To gain a relatively high temporal resolution, we used line scans at rates of 100–150 Hz. We imaged neurons at depths of 250–380 μm below the surface of the brain, corresponding to cortical layers 2/3 (Rothschild et al., 2010). We imaged sequentially at multiple depths in each mouse, simultaneously imaging an average of 9 $\pm$ 4 neurons that passed the quality threshold in each focal plane (Fig. 1).

Single neuron response profiles after parturition

To test how synthetic as well as natural sounds are coded in A1 of mice after parturition, we presented eight different auditory stimuli, comprised of three different pure tones (10, 20, and 60 kHz), BBN, a synthetic wriggling call (WC, composed of pure tones at 3.8, 7.6, and 11.4 kHz) (Ehret, 2005), and three USVs (recorded from 4- to 5-d-old pups). During continuous imaging

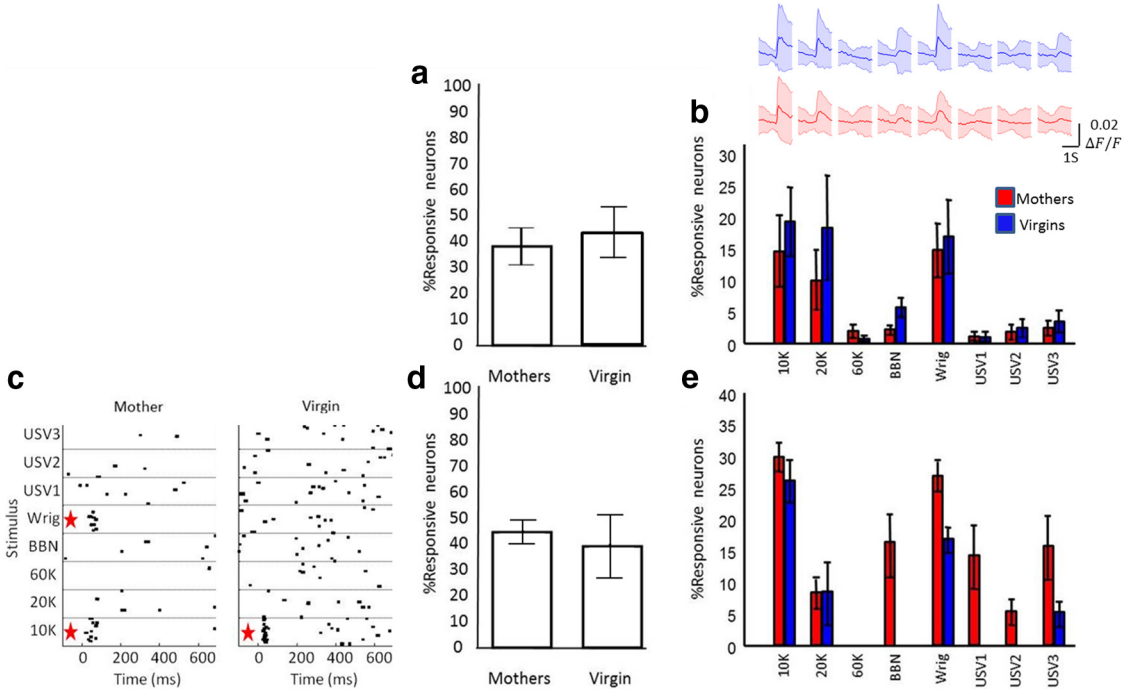

Figure 2. Responsiveness of single cells in A1 of mothers and virgins. ***a***, Percentage of responsive neurons in mothers and virgins across imaging experiments. ***a***, ***b***, Error bars indicate SEM. ***b***, Mean per-stimulus responses (top) and responsiveness rate (bottom) in mothers (red) and virgins (blue). Shaded area marks SD across data; error bars indicate SEM across experiments. ***c***, Representative raster plots from juxtacellular electrophysiological recordings of L2/3 neurons in a mother (left) and virgin (right). Each stimulus (noted on the left) was presented 20 times. Stimulus onset is at time 0. Red stars indicate significant responses. ***d***, Percentage of responsive neurons in mothers (left) and virgins (right), as determined from the electrophysiological recordings. Compare with ***a***, which was obtained from different animals using two-photon calcium imaging. ***e***, Per-stimulus responsiveness in mothers (red) and virgins (blue), as determined from the electrophysiological recordings. Compare with ***b***, which was obtained from different animals using two-photon calcium imaging.

of each focal plane, we presented each stimulus 20 times for a total of 160 stimuli presentations, in a pseudo-random sequence. Neurons exhibited stimulus-evoked as well as spontaneous calcium transients with a characteristically fast rise time (~100 ms) and a slow exponential decay (500–1000 ms) (Fig. 1*b*,*c*,*e*,*f*). As the area under the fluorescence transients correlates with the number of fired spikes (Abel et al., 2004; Kerr et al., 2005; Yaksi and Friedrich, 2006; Sato et al., 2007; Sasaki et al., 2008; Tian et al., 2009; Rothschild et al., 2010), response amplitudes were defined as the integral of the ΔF/F signal from 0 to 250 ms after stimulus onset. Overall, in both mothers and virgins, some neurons showed high stimulus selectivity (Fig. 1*f*; cell 7/10 kHz), whereas others were less selective (Fig. 1*c*; cell 1). Response consistency over trials varied greatly between neurons and stimuli (see, e.g., Fig. 1*c*; cell 5, 60 K, WC, and BBN). As we previously described (Rothschild et al., 2010), neurons within the imaged region could show similar or highly divergent stimulus selectivity (Fig. 1*c*; cells 1 and 3 vs 1 and 7; stars indicate significant responses).

We defined a responsive neuron as one that responded significantly to at least one stimulus. Of all neurons in lactating mothers ($n = 418$ neurons; $N = 6$ mice) and virgin mice ($n = 283$ neurons; $N = 9$ mice), a mean ± SEM of 37.7 ± 7.4% and 41.9 ± 9.6% of neurons were responsive per animal. There was no significant difference in the fraction of responsive neurons between the two groups when grouping by animals (two-sample t test, df = 13, $p = 0.76$; Fig. 2*a*). When pooling all neurons for each experimental group, responsiveness tended to be higher in virgins, although this difference did not reach significance (two-sample t test, df = 699, $p = 0.052$). Thus, the overall responsiveness of imaged A1 neurons in L2/3 to this stimulus set was comparable in naive virgins and lactating mothers.

We next examined whether neurons in mothers displayed a different stimulus selectivity compared with virgins. The mean response profile of mothers and virgin mice did not differ significantly (two-way ANOVA on state × stimuli, no significant effect of state: $F_{(1,111)} = 1.44$, $p = 0.24$; significant effect of stimulus: $F_{(7,111)} = 6.93$, $p < 0.0001$; no interaction between state and stimuli: $F_{(7,104)} = 0.28$, $p = 0.96$; Fig. 2*b*). In both groups, more neurons were responsive to 10 and 20 kHz tones, and to synthetic wriggling calls, whereas few neurons were responsive to USVs, BBN, and the 60 kHz tones. The lack of responses to USVs and 60 kHz tones and high rate of responses to 10 and 20 kHz tones and wriggling calls are explained by consistent imaging from central A1. The low rate of responses to BBN is a unique feature of layer 3 neurons, which probably dominate our imaging sample (Oviedo et al., 2010). Thus, within the sample of sounds we presented, we found no differences in the mean response properties of single neurons in mothers and virgin mice in our imaging data.

Compared with electrophysiology, two-photon calcium imaging yields a lower signal-to-noise ratio for measuring spiking activity and suffers from a limited temporal resolution. To ensure that our results are comparable with direct electrophysiological measures, we performed electrophysiological recordings from limited samples in mothers ($N = 59$ neurons from 4 mice) and virgin mice ($N = 34$ neurons from 4 mice). Recordings were made in the cell-attached configuration, which allows excellent single-neuron and single-spike identification. We recorded from the same stereotaxic coordinates as in our imaging experiments, and aimed our recordings to depths corresponding to L2/3 as in our imaging experiments. We presented the exact same auditory protocol and performed similar analysis to that of the imaging data (with the required modifications for the different signals, see Materials and Methods). Raster plots of representative neurons

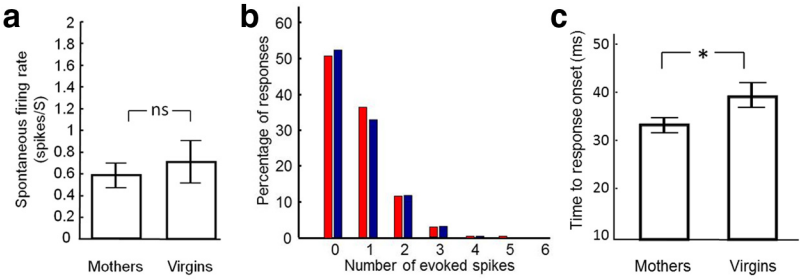

Figure 3. Firing properties of neurons in virgins and mothers. ***a***, Spontaneous firing rates from all mothers and virgins. Error bars indicate SEM. ***b***, Distribution of number of stimuli-evoked spikes in mothers (red) and virgins (blue). Spikes within 1–100 ms from stimuli onset were considered stimulus-evoked. ***c***, Time to response onset in mothers and virgins. Error bars indicate SEM. *$p = 0.036$ (two-way t test). ns, Not significant.

from a mother mouse and a virgin mouse are presented in Figure 2*c*. As with the imaging data, stimulus selectivity and intertrial variability varied greatly between neurons. Using the same responsiveness test as for the imaging data, a mean ± SEM of 44 ± 4.7% of all neurons in mothers and 38.8 ± 13.2% of the neurons in virgins were responsive to at least one stimulus, which is consistent with the values obtained from the imaging data (compare Fig. 2*a*,*d*). Per-stimulus responsiveness was similar, although not identical, to that derived from the imaging data. The stimuli that evoked most responses were the low-frequency tones (10 and 20 kHz) and the wriggling calls, consistent with the recording location in the center of A1 (Fig. 2*e*, compare withFig. 2*b*). However, BBN and the USVs evoked more electrophysiological responses in mothers than could be expected based on the imaging data. These differences are probably the result of small differences in the recorded neuronal populations because of different biases of the techniques (see Discussion).

Beyond complementing our imaging results, electrophysiological recordings allowed us to study single-neuron activity in more detail. First, we calculated the spontaneous firing rate of all neurons over the 100 ms preceding each stimulus presentation. Spontaneous firing rates in L2/3 were overall low and not significantly different between mothers and virgins (virgins, 0.69 ± 0.21 Hz; mothers, 0.59 ± 0.11 Hz, mean ± SEM; Fig. 3*a*, two-sample t test, df = 91, $p = 0.64$). Second, we examined whether the amplitude of auditory evoked responses differed between mothers and virgins by quantifying the number of evoked spikes for all trials of response-evoking stimuli. The distribution of number of evoked spikes per trial was similar for mothers and virgins (Fig. 3*b*), and their means were not significantly different (two-sample t test, df = 1838, $p = 0.52$). In ~50% of the trials, there were no spikes within the response window, and in >95% of the trials responses consisted of no more than two spikes, in both mothers and virgins. Last, we examined spike-timing differences in virgins and mothers. Interestingly, response onset in mothers preceded those of virgins by ~6 ms (Fig. 3*c*; virgins, 39.2 ± 2.4 ms; mothers, 32.9 ± 1.7 ms, mean ± SEM; two-sample t test, df = 39, $p = 0.036$). Thus, our electrophysiological data generally support the similarity of responses in mothers and virgins we observed using calcium imaging.

Pairwise NC after parturition

One basic measure for network dynamics is pairwise NC. NC measures the tendency of two neurons to respond above and below their means ("fluctuate") together, and it has been shown to correlate with synaptic connectivity (Ko et al., 2011). Figure 4*a* shows an example of fluctuation vectors (see Materials and Methods) for two neurons imaged simultaneously that showed a strong tendency to cofluctuate. These neurons were imaged from a mother. The tendency of this pair to cofluctuate is illustrated again in Figure 4*b*, showing a scatter plot of the fluctuations of one neuron against the fluctuations of the other. NC in this case is extremely high (NC = 0.77). In contrast, Figure 4, *c* and *d*, show the same analyses for a pair with low NC (NC = 0.008) from a virgin animal.

Across our dataset, the average NC in virgin mice was 0.18 ± 0.14 (mean ± SD, $n = 1103$ pairs), consistent with our previous results (Rothschild et al., 2010). Remarkably, mean NC in lactating mothers was almost twice as high compared with virgins (0.34 ± 0.17, $n = 2148$ pairs), and this difference was highly significant (Fig. 4*e*; two-sample t test, $t = 27.8$, df = 3249, $p < 0.01$). These unusually high NC values in mothers were consistent across individual animals (data not shown). Pairwise correlations during ongoing activity, when no stimuli were presented, were also significantly higher in mothers (Fig. 4*f*; two-sample t test, $t = 8.1$, df = 3249, $p < 0.01$). However, this difference was smaller than the difference we found for stimulus-evoked NCs.

The finding that stimulus-evoked NC values in mothers were on average twice as large as in virgins prompts the question of whether this difference originates from responses to a specific subset of stimuli, which might be coded differently in mothers. We therefore calculated stimulus-specific NC in mothers and virgins (see Materials and Methods). For both mothers and virgins, NC varied significantly with stimulus identity (Fig. 4*g*, ANOVA: mothers, $F_{(7,17176)} = 14.32$, $p < 0.001$; virgins, $F_{(7,8816)} = 4.85$, $p < 0.0001$). However, the magnitude of variation of NC with stimuli across the dataset was small (SD/mean NC across stimuli was 0.063 for mothers and 0.097 for virgins). USVs and WCs did not induce differential levels of NC compared with pure tones, and NCs were larger in mothers for all stimuli. These results indicate that the increased NC in mothers included a large stimulus-independent component.

To test how sensitive our results are to the response window size (250 ms), we recalculated both responsiveness rates and NC values based on four additional response window sizes (10, 100, 500, and 800 ms; Fig. 5*a*). Mean response profiles in both mothers and virgins were very similar when using a shorter window of 100 ms (Fig. 5*b*), as well as when taking the maximal ΔF/F value rather than the integral (Fig. 5*c*). Most importantly, NC values were similar for all window durations between 100 and 800 ms windows (Fig. 5*d*).

High-order correlations after parturition

To analyze high-order NCs, we grouped fluctuation vectors of all simultaneously imaged neurons into "fluctuation matrices." In each matrix, each row describes the fluctuations of one neuron to all 160 individual trials, ordered chronologically. Representative fluctuation matrices from three virgin mice and three lactating mothers are shown in Figure 6, *a* and *b* (top). The strong tendency of multiple neurons to cofluctuate is evident in the data from lactating mothers as brighter or darker vertical lines in the fluctuation matrices, indicating that in a given trial a large fraction of the neurons fluctuated up/down together. Qualitatively, population fluctuations were less pronounced in the matrices from

virgin mice. The mean fluctuation, averaged across all neurons in each trial, had an approximate Gaussian distribution centered on 0 in the virgin mice data (Fig. 6*a*, middle and bottom). In contrast, the average fluctuations in mothers were skewed to the right (Fig. 6*b*, middle and bottom).

The increased correlations in the population (and the concomitant larger average fluctuations across the population) could result in principle from two nonmutually exclusive effects. First, it could be that in mothers, once common fluctuations occurred between a pair of neurons, these fluctuations would tend to be larger than in virgins, leading to a larger covariances and therefore larger correlations. Second, it could be that in mothers, once a common fluctuation occurred, it involved more neurons than in virgins, leading to a larger number of significant pairwise correlations. To dissociate the effects of fluctuation size and number of cofluctuating neurons, we calculated the sizes of cofluctuations in pairs of neurons (quantified by the product of the deviations of the two neurons from their individual average responses to the stimulus), conditioned on the number of neurons that had a positive fluctuation (response above their average, termed here "activated neurons") in each trial. The size of the pairwise cofluctuation increased with the number of activated neurons. For example, in Figure 6*c*, we quantified the probability of having a large cofluctuation (>0.1) as a function of the number of activated neurons in the group. Importantly, conditioned on the number of activated neurons, the size of the cofluctuations was similar at least up to $n = 9$ activated neurons (Kolmogorov–Smirnov test, $p > 0.05$, corrected for multiple comparisons). The differences between the two groups for trials that had a larger number of activated neurons were not individually significant because there were only a small number of trials with so many activated neurons.

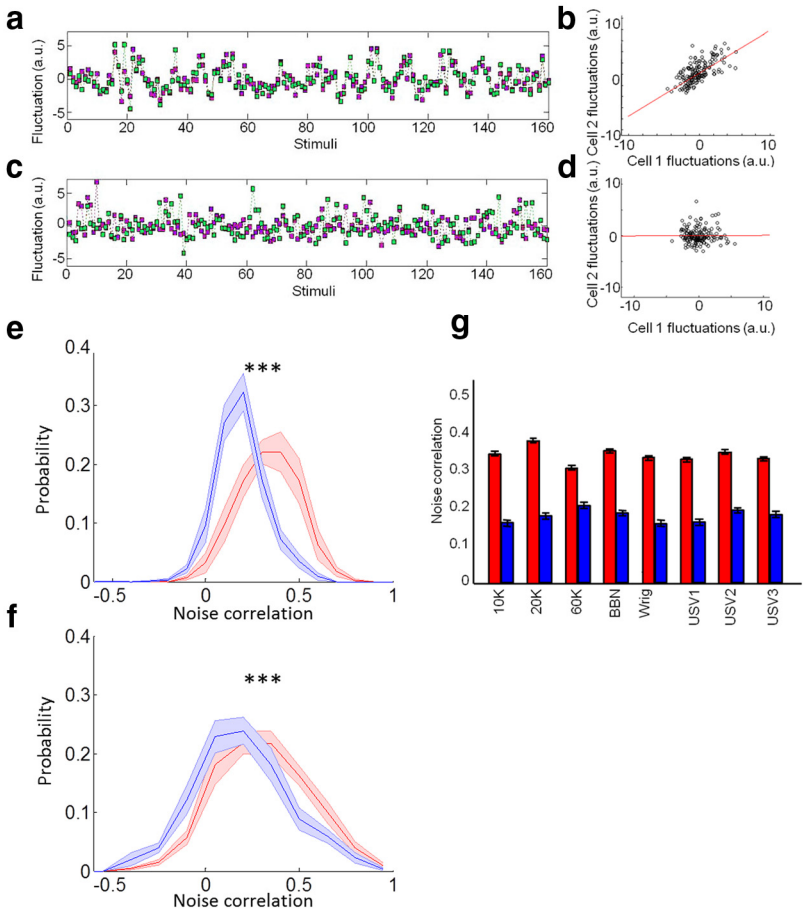

Figure 4. NCs between pairs of neurons in A1 of mothers and virgins. ***a***, Response fluctuations during the presentation of 160 individual stimuli for one neuronal pair from a mother with high positive NC (NC = 0.77). ***b***, Scatter plot of the fluctuations of one neuron from (***a***) against the corresponding fluctuations of the second neuron. ***c***, ***d***, Same as ***a*** and ***b*** but for a pair of neurons with low NC (NC = 0.008) from a virgin animal. ***e***, Distribution of NC values in mothers (red) and virgins (blue). Shaded areas are SEM across experiments. Mean NC in mothers (0.34) is significantly higher compared with that of virgins (0.18). ***$p < 0.001$. ***f***, Distribution of NC values during ongoing activity (no stimuli) in mothers (red) and virgins (blue). Shaded areas are SEM across experiments. Mean NC in mothers (0.31) is significantly higher compared with that of virgins (0.24). ***$p < 0.001$. ***g***, Stimulus-specific NC in mothers (red) and virgins (blue).

Having shown that, conditioned on the number of activated neurons, fluctuation sizes are not different in mothers and in virgins, we are left with the possibility that in mothers larger groups of neurons tended to be activated together. To quantify these high-order correlations independently of fluctuation size, we first quantified fluctuations to positive or negative (±1). This resulted in population fluctuation vectors (or "patterns"), where a +1/−1 corresponded to a neuron fluctuating above/below its average, respectively. We compared the probability of these population fluctuation patterns with a model with independent fluctuations across neurons. For each subset of N-imaged neurons, we calculated the expected probability that all neurons of the subset simultaneously responded above their average response (ignoring neurons outside that subset) based on an independent model and compared it with the actual observed rate (see Materials and Methods). Figure 6*d* (top left) shows such an analysis for one set of nine neurons imaged in a virgin mouse (same data as Fig. 6*a*, middle column), and Figure 6*d* (top right) shows an example of 12 neurons from a mother (same data as Fig. 6*b*, middle column). The color code indicates the size of the subset. For example, the green dots in the upper right corner indicate single-cell activation patterns, and by construction their observed rates are identical to the expected rates. For patterns with two or more active neurons, virtually all activation patterns occurred more often than expected by an independent model. These high-order NCs were eliminated by shuffling responses of the neurons between trials (Fig. 6*d*, bottom panels). Whereas patterns occurring more often than expected by the independent model were evident in both mothers and virgins, the ratio of observed/expected patterns was much higher in mothers. Many patterns of activation in mothers occurred 200–2000 times more often than expected (Fig. 6*e*). Thus, correlated fluctuations of large neuronal populations were prevalent in A1 of mothers.

Decoding stimulus identity from ensemble activity

Last, we examined the effect of NCs in virgins and mothers on stimulus decoding. We asked how well an observer could decode stimulus identity from ensemble activity patterns in mothers and virgins. To measure classification performance of neurons re-

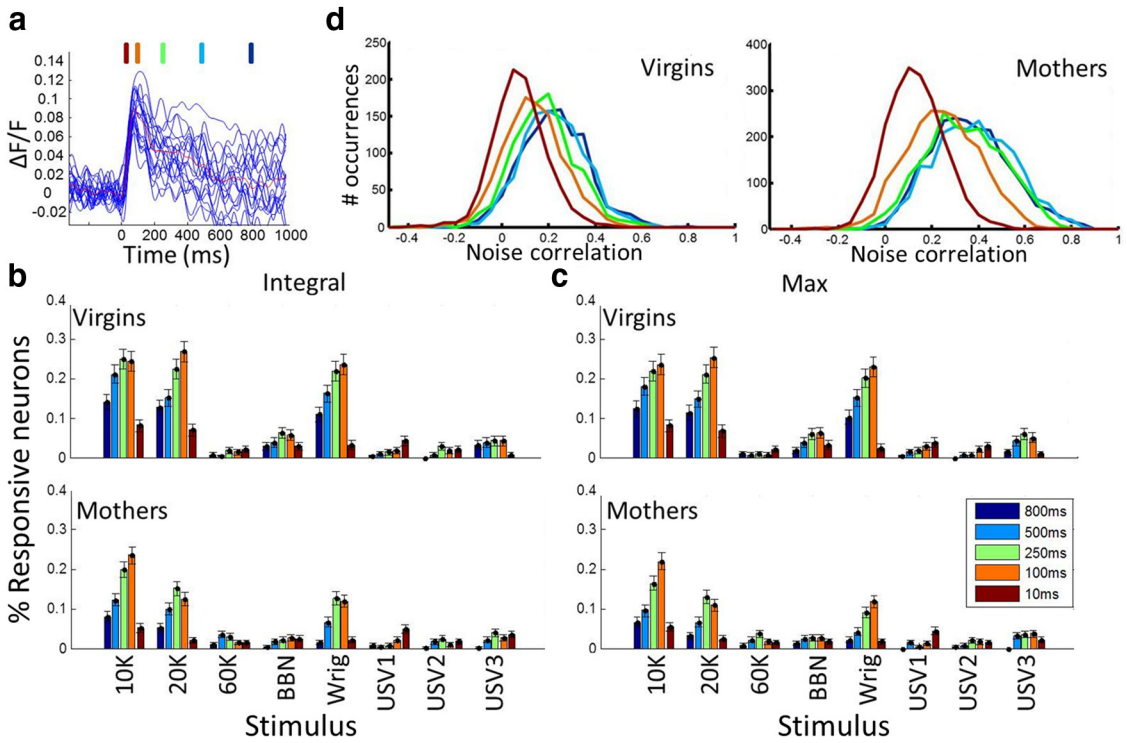

Figure 5. Responsiveness and NC measures are stable across temporal integration windows. ***a***, Example calcium transients of one neuron evoked by multiple presentations of a single stimulus. Colored lines on top indicate the response window used in this study (250 ms, green), and four additional window sizes assessed here: 10 ms, dark brown; 100 ms, light brown; 500 ms, light blue; and 800 ms, dark blue. Color legend for all panels in ***c***. ***b***, Per-stimulus responsiveness in virgins (top) and mothers (bottom) assessed using different response window sizes. Error bars indicate SEM across the data. ***c***, Same as ***b***, but using the maximum rather than the integral over the response window. ***d***, Distribution of NC values in virgins (left) and mothers (right) across different response window sizes.

corded simultaneously in an imaging session, we performed linear discriminant analysis on the ensemble response patterns using a leave-one-out procedure. To determine chance performance, we shuffled the responses of each imaging session between stimuli 100 times. Classification performance was quantified as percentage loss, which is the rate of incorrectly classified patterns (good performance corresponds to small percentage loss).

Performance in both mothers and virgins was not high but was better than chance in most ensembles (Fig. 7*a*). Performance did not differ between mothers and virgin mice (% loss mean ± SD: virgins, 61.8 ± 6.4%; mothers, 64.5 ± 9.5, two-sample *t* test, $t = 1.38$, $p = 0.17$, df = 68). Furthermore, there was no significant correlation between NC and classification performance in virgins (Fig. 7*b*, left; $r = 0.18$, $p = 0.33$, df = 30) or mothers (Fig. 7*b*, right; $r = 0.09$, $p = 0.6$, df = 36). Thus, ensembles with larger NCs did not show a consistently different classification performance than ensembles with lower NCs.

We next assessed the effect of NCs on the classification performance of neurons within each recording session individually. To this end, we eliminated NCs by pseudo-randomly shuffling the responses of each neuron among trials with the same stimulus type 100 times and analyzing the trial-shuffled data in the same manner (Fig. 7*c*). There was no significant effect of NC on the difference between real data performance and NC-eliminated data performance in virgins (Fig. 7*d*, left; $r = 0.12$, $p = 0.52$, df = 30) or mothers (Fig. 7*d*, right; $r = -0.24$, $p = 0.14$, df = 36).

For virgin mice, eliminating NC did not significantly change classification performance in 30 of 32 ensembles (93.75%), whereas in 2 of 32 ensembles (6.25%) elimination of NCs significantly improved performance (two-sample *t* test per ensemble between performance of original data and performance of 100 trials of NC-eliminated data, df = 100). For mothers, eliminating NC did not significantly change classification performance in 33 of 38 ensembles (86.84%), significantly improved performance in 3 of 38 ensembles (7.89%), and significantly lowered performance in 2 of 38 ensembles (5.26%) (two-sample *t* test per ensemble between performance of original data and performance of 100 trials of NC-eliminated data, df = 100). Thus, overall, eliminating NC did not have a systematic effect on classification performance in either group, despite the substantially larger NCs in mothers.

Discussion

We used *in vivo* two-photon calcium imaging of L2/3 neurons in A1 of lactating mothers and virgin mice to study how the difference between these groups is expressed in the activity of local neural populations. Under our recording conditions, single-neuron response properties were generally similar between virgins and mothers, whereas pairwise and higher-order correlations were considerably higher in mothers.

Mothers and virgin mice differed by two main factors: experience and physiological state. By the time of imaging and recording, mothers had mated, undergone pregnancy and birth, and then spent 4–5 d of maternal care with the pups. This process does not only expose the mother mice to an enriched environment but also involves a learning process, especially because these were first-time mothers. In addition, during pregnancy and after parturition, the neuro-endocrinological state of mothers undergoes large changes, which may have profound effects on sensory processing (Brunton and Russell, 2008). It is thus likely that a combination of internal physiological processes and experience modulates neural activity in A1 of mothers.

Our data were acquired from anesthetized animals, in which imaging of auditory cortex is straightforward. Obviously, experience- or learning–dependent changes should ultimately be tested in awake

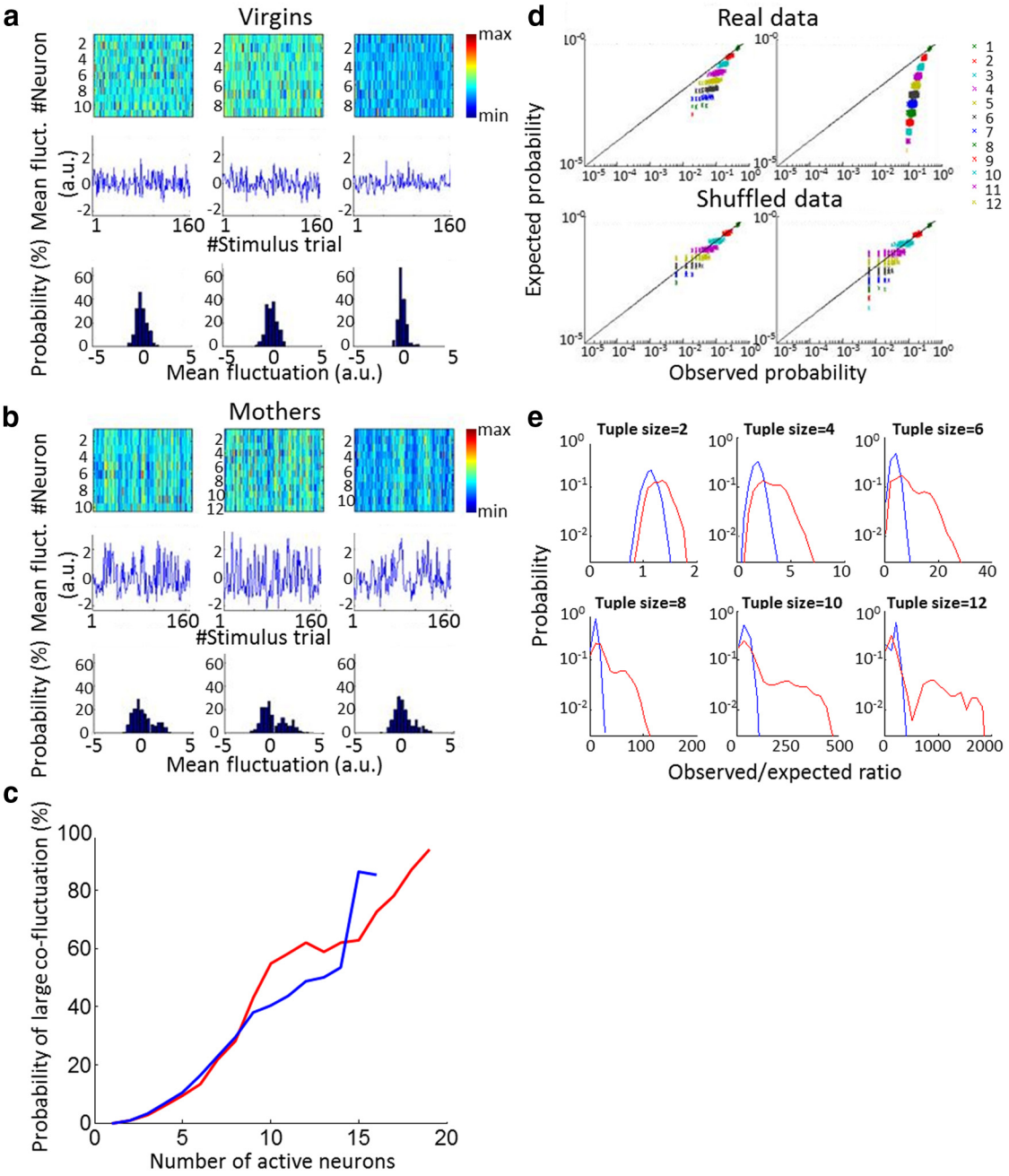

Figure 6. Higher-order correlations in virgins and mothers. ***a***, Fluctuation matrices from three representative recordings from virgins (top panels), the corresponding mean population fluctuations (middle panels), and the distributions of population fluctuations (bottom panels). ***b***, Same as ***a*** but for three representative recordings from mothers. ***c***, Probability of large cofluctuations (>0.1) as a function of a number of activated neurons. ***d***, Expected probability based on an independent model as a function of observed probability of population activation patterns for a representative recording from a virgin (top left) and from a mother (top right). Color codes the size of the subset. Observed probabilities are higher in both virgins and mothers, but this trend is stronger in mothers. Bottom panels, The same analysis as the corresponding top panels but for trial-shuffled data. For shuffled data, on average patterns were observed at expected rates from an independent model because correlations were eliminated. ***e***, Distribution of observed/expected probabilities from the mother (red) and virgin (blue) data, for different tuple sizes. For large tuple sizes, observed/expected rates were substantially larger for mothers.

animals. Anesthesia can affect single-neuron response properties (Cheung et al., 2001; Gaese and Ostwald, 2001; Haider et al., 2013) as well as neuronal correlations (Movshon et al., 2003; Rennaker et al., 2007; Greenberg et al., 2008). In particular, we cannot rule out a differential effect of anesthesia on mothers and virgin mice, although we find this possibility unlikely.

Single-neuron changes

In a previous electrophysiological study comparing responses of single cells in A1 of mothers and virgins, responses to USVs in mothers were found to carry more information compared with those of virgins (Liu and Schreiner, 2007). Consistent with our imaging and electrophysiological results, the authors found no differences in response probability, response amplitude, or mean frequency tuning between mothers and virgins. The changes in the level of NCs described here parallel and complement the findings of Liu and Schreiner (2007): it is conceivable that the larger NCs we describe here can interact with the higher information content found by Liu and Schreiner (2007) to generate more efficient readout of the sensory information.

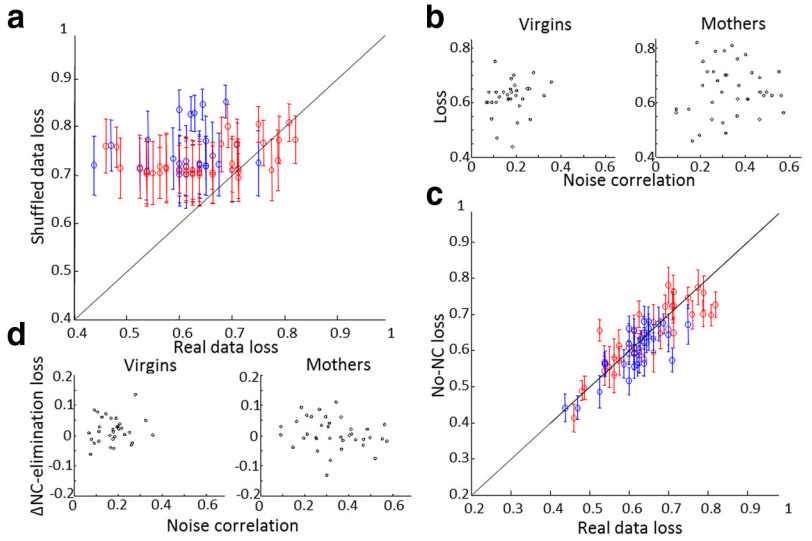

Figure 7. Classification and NC in mothers and virgin mice. ***a***, Shuffled data loss as a function of real data loss. Error bars indicate SD of 100 shuffles. Red represents ensembles from mothers; blue represents ensembles from virgins. Real data have lower loss than shuffled data in the majority of ensembles. ***b***, Classification loss as a function of NC in virgins (left) and mothers (right). ***c***, Classification loss of NC-eliminated data as a function of real data. Error bars indicate SD of 100 trial shuffles. Color code as in ***a***. ***d***, Classification loss–NC eliminated loss as a function of NC in virgins (left) and mothers (right).

A recent electrophysiological study by some of us, using loose-patch recordings from A1 of mothers found that overall responsiveness, and specifically responsiveness to USVs, is enhanced in mothers (Cohen et al., 2011). Clearly, the imaging data in the current study did not show a comparable change. We suspected that the discrepancy between these results stems from the difference in recording depth, as response properties in A1 show dependence on cortical layer (Sakata and Harris, 2009; Oviedo et al., 2010). Although most neurons in the previous study were recorded from deep cortical layers, the neurons imaged here were from layers 2/3. To test this possibility, we performed electrophysiological recordings and presented the same auditory protocol as in the imaging experiments, while limiting recording depth to superficial layers. Whereas responsiveness rates of virgins were similar using the two techniques (compare Fig. 2*b*,*e*, blue bars), responsiveness in mothers was still generally higher in the electrophysiological data compared with the imaging data (compare Fig. 2*b*,*e*, red bars). However, the electrophysiologically measured responsiveness rates reported here from layers 2/3 of mothers were substantially lower than those observed in deeper layers, as reported in Cohen et al. (2011). In that study, 40% of neurons in mothers were responsive to USVs, whereas in our current recordings from superficial layers this rate was 22%. This suggests that recording depth at least partially accounts for the difference in responsiveness rates observed in mothers using the different techniques. There are a number of possible explanations for the remaining discrepancy between the imaging and electrophysiological responsiveness rates. First, although our imaging data were strictly from L2/3, the electrophysiological data may contain neurons at more variable depths because we did not verify soma positions in our blind recordings. Second, fast spiking interneurons, which have been shown to undergo unique changes in mothers (Cohen et al., 2011) may be under-represented in the imaging dataset because of inferior signal-to-noise ratio of their spike-evoked fluorescence transients (Nauhaus et al., 2012). Last, identification of single spikes with calcium imaging involves a small but positive error rate, and we cannot rule this out as a possible factor. The exact biases of electrophysiology and imaging remain to be further evaluated.

Previous studies on learning-induced changes in NC

Parturition and taking care of the pups is a complex and unique life event, and previous studies have not studied its effect on cortical network dynamics. However, these events share some features with sensory enrichment and experimental learning paradigms.

In a previous study, ensemble activity in A1 of awake monkeys was recorded while training on a tone discrimination task (Ahissar et al., 1992). The results showed that correlation between pairs of neurons could strongly increase during learning and remained at an increased level as long as no additional manipulations were performed. Whereas this effect was dependent on spike-timing conditioning, it was also dependent on behavior, highlighting the importance of behavioral relevance for inducing functional plasticity. This study revealed the potential of auditory cortical networks to increase their functional connectivity by driving pairs of neurons to fire at short succession. Our results indicate that such increases in functional connectivity occur during a natural life event as well.

A more recent study implemented *in vivo* two-photon calcium imaging in the motor cortex of behaving rats while they were learning a discrimination task (Komiyama et al., 2010). The authors found that correlation between pairs of neurons increased throughout learning and suggested that correlated activity in specific ensembles of functionally related neurons is a signature of learning-related circuit plasticity.

The most direct support for experience-dependent changes of interneuronal correlations in auditory cortex comes from a recent study in songbirds (Jeanne et al., 2013). In this study, associative learning of specific auditory motifs and reward location led to changes in interneuronal correlations in auditory cortex. These data support our result that correlation patterns in auditory cortex are experience dependent and highlight the neural population level as a key neural substrate of learning.

Possible mechanisms of NC increase

NC has traditionally been attributed to common input or direct connectivity between a pair of neurons (Moore et al., 1970; Lytton and Sejnowski, 1991; Shadlen and Newsome, 1998; Morita et al., 2008). Indeed, a recent study found a significant correlation between the NC of pairs of neurons and the probability of synaptic connectivity between them (Ko et al., 2011). Neurons within our imaging window were at distances of 0–200 μm from each other, and the probability of direct synaptic connections and receiving common input is highest at such distances (Song et al., 2005; Ko et al., 2011; Perin et al., 2011; Levy and Reyes, 2012). These findings suggest that NC in our data may reflect the strong recurrent connectivity of the local cortical network.

If NC reports synaptic connectivity, what process underlies the increased level of NC we observed in mothers? Changes in NC have previously been reported mostly after momentary changes in attention, stimuli, or behavior, on timescales of seconds or

minutes (Ahissar et al., 1992; Vaadia et al., 1995; Cohen and Newsome, 2008; Gutnisky and Dragoi, 2008; Cohen and Maunsell, 2009; Mitchell et al., 2009). Although the mechanism for these changes is largely unknown, it has been suggested that context-dependent changes in neuromodulation of the recorded neurons or their input may account for changes in NC (Brunel and Wang, 2001; Belitski et al., 2008; Joshua et al., 2009; Thiele et al., 2012). As motherhood involves changes in neuromodulation (Brunton and Russell, 2008; Leuner et al., 2010), these changes may account for the increased NC we observed.

However, our findings differ in a few important aspects from most of the above studies. First, becoming a mother involves a much longer time scale, of days and weeks, after which we observed the high NC. Moreover, the differences in NC levels were largely insensitive to stimuli and did not involve attention or action. This may suggest that a slower and more "hardwired" mechanism accounts for our results. There is now much evidence for experience-dependent synaptic plasticity in adulthood (for review, see Holtmaat and Svoboda, 2009; Fu and Zuo, 2011). Interestingly, some recent studies describe a net increase in the number of synaptic connections after sensory experience and learning (Xu et al., 2009; Yang et al., 2009). Sensory enrichment or deprivation can also induce a fast increase in the amount of synapses in various brain regions (Moser et al., 1994; Knott et al., 2002; Hofer et al., 2009; Holtmaat and Svoboda, 2009; Bose et al., 2010). Although these studies did not include physiological recordings, the increased synaptic connectivity is likely to result in an increase in NC.

In the days after parturition, mother mice are exposed to novel sensory stimuli and undergo a learning process that is at least as striking as those used in these studies. It is thus possible that our finding of elevated NCs in mothers reflect a network-physiological correlate of experience- and learning-induced increase in synaptic connections.

Computational implications

Although NCs have been reported between pairs of cortical neurons in a large number of studies (Ahissar et al., 1992; Zohary et al., 1994a; Vaadia et al., 1995; Bair et al., 2001; Kohn and Smith, 2005; Cohen and Newsome, 2008; Cohen and Maunsell, 2009; Mitchell et al., 2009; Cafaro and Rieke, 2010; Komiyama et al., 2010; Ohiorhenuan et al., 2010; Rothschild et al., 2010), their role in network computation is not fully understood. Positive average NCs may have a detrimental effect on coding efficiency under some assumptions about the way information is "read out" from a population of neurons (Zohary et al., 1994a; Sompolinsky et al., 2001), but in conjunction with natural assumptions about response variability, they may leave coding efficiency unaffected or even improve it (Abbott and Dayan, 1999; Averbeck and Lee, 2006; Shamir and Sompolinsky, 2006; Cafaro and Rieke, 2010).

We studied coding efficiency by measuring how well stimulus identity could be decoded from ensemble activation patterns in mothers and virgin mice, and we examined the effect of NC on decoding performance. Remarkably, we found that NCs did not have a systematic effect on decoding, despite being twice as high in mothers. Eliminating correlations by shuffling did not have a net effect on decoding either. Last, there was no correlation between the mean NC level within an ensemble and its decoding performance. These findings indicate that NCs represent a component of the response that is functionally "orthogonal" to the stimulus-related information in that stimulus identity seems to be as well coded by cortical ensembles both in the presence and in the absence of high NCs.

This result puts into sharp relief the question of the role of NCs in cortical computations and, in particular, the role subserved by the higher correlations in mothers. One possibility is that, rather than optimizing stimulus classification, L2/3 neurons optimize transmission efficiency to downstream regions. In support of this alternative, it has been shown that pairwise correlations are expected to increase the variability of the population output spike train to downstream regions (Salinas and Sejnowski, 2000). Our data are consistent with this finding, as increased correlations in mothers resulted in a more bimodal distribution of mean population events (Fig. 6*a*,*b*). A different possibility is that higher correlations do not improve coding but are rather a temporary transition phase reflecting network reorganization. Previous studies on experience-dependent increases in synaptic connections show that the initial increase in the days after experience returns to baseline in the following weeks (Knott et al., 2002; Holtmaat and Svoboda, 2009; Xu et al., 2009; Yang et al., 2009). It has been suggested that this initial net increase in synaptic connections allows the network to restructure. Whether the increased correlation we observed in mothers is a manifestation of such a process could be tested in future studies by applying recent technological advances to monitor neuronal ensembles at multiple time points throughout pregnancy, parturition, and the weeks thereafter.

References

Abbott LF, Dayan P (1999) The effect of correlated variability on the accuracy of a population code. Neural Comput 11:91–101. CrossRef Medline

Abel HJ, Lee JC, Callaway JC, Foehring RC (2004) Relationships between intracellular calcium and afterhyperpolarizations in neocortical pyramidal neurons. J Neurophysiol 91:324–335. CrossRef Medline

Ahissar E, Vaadia E, Ahissar M, Bergman H, Arieli A, Abeles M (1992) Dependence of cortical plasticity on correlated activity of single neurons and on behavioral context. Science 257:1412–1415. CrossRef Medline

Averbeck BB, Lee D (2006) Effects of noise correlations on information encoding and decoding. J Neurophysiol 95:3633–3644. CrossRef Medline

Bair W, Zohary E, Newsome WT (2001) Correlated firing in macaque visual area MT: time scales and relationship to behavior. J Neurosci 21:1676–1697. Medline

Bakin JS, Weinberger NM (1990) Classical conditioning induces CS-specific receptive field plasticity in the auditory cortex of the guinea pig. Brain Res 536:271–286. CrossRef Medline

Belitski A, Gretton A, Magri C, Murayama Y, Montemurro MA, Logothetis NK, Panzeri S (2008) Low-frequency local field potentials and spikes in primary visual cortex convey independent visual information. J Neurosci 28:5696–5709. CrossRef Medline

Bose M, Muñoz-Llancao P, Roychowdhury S, Nichols JA, Jakkamsetti V, Porter B, Byrapureddy R, Salgado H, Kilgard MP, Aboitiz F, Dagnino-Subiabre A, Atzori M (2010) Effect of the environment on the dendritic morphology of the rat auditory cortex. Synapse 64:97–110. CrossRef Medline

Brunel N, Wang XJ (2001) Effects of neuromodulation in a cortical network model of object working memory dominated by recurrent inhibition. J Comput Neurosci 11:63–85. CrossRef Medline

Brunton PJ, Russell JA (2008) The expectant brain: adapting for motherhood. Nat Rev Neurosci 9:11–25. CrossRef Medline

Cafaro J, Rieke F (2010) Noise correlations improve response fidelity and stimulus encoding. Nature 468:964–967. CrossRef Medline

Cheung SW, Nagarajan SS, Bedenbaugh PH, Schreiner CE, Wang X, Wong A (2001) Auditory cortical neuron response differences under isoflurane versus pentobarbital anesthesia. Hear Res 156:115–127. CrossRef Medline

Cohen L, Rothschild G, Mizrahi A (2011) Multisensory integration of natural odors and sounds in the auditory cortex. Neuron 72:357–369. CrossRef Medline

Cohen MR, Maunsell JH (2009) Attention improves performance primarily by reducing interneuronal correlations. Nat Neurosci 12:1594–1600. CrossRef Medline

Cohen MR, Newsome WT (2008) Context-dependent changes in functional circuitry in visual area MT. Neuron 60:162–173. CrossRef Medline

Ehret G (2005) Infant rodent ultrasounds: a gate to the understanding of sound communication. Behav Genet 35:19–29. CrossRef Medline

Fritz J, Shamma S, Elhilali M, Klein D (2003) Rapid task-related plasticity of spectrotemporal receptive fields in primary auditory cortex. Nat Neurosci 6:1216–1223. CrossRef Medline

Fu M, Zuo Y (2011) Experience-dependent structural plasticity in the cortex. Trends Neurosci 34:177–187. CrossRef Medline

Gaese BH, Ostwald J (2001) Anesthesia changes frequency tuning of neurons in the rat primary auditory cortex. J Neurophysiol 86:1062–1066. Medline

Geissler DB, Ehret G (2002) Time-critical integration of formants for perception of communication calls in mice. Proc Natl Acad Sci U S A 99: 9021–9025. CrossRef Medline

Geissler DB, Ehret G (2004) Auditory perception vs. recognition: representation of complex communication sounds in the mouse auditory cortical fields. Eur J Neurosci 19:1027–1040. CrossRef Medline

Greenberg DS, Houweling AR, Kerr JN (2008) Population imaging of ongoing neuronal activity in the visual cortex of awake rats. Nat Neurosci 11:749–751. CrossRef Medline

Gutnisky DA, Dragoi V (2008) Adaptive coding of visual information in neural populations. Nature 452:220–224. CrossRef Medline

Haider B, Häusser M, Carandini M (2013) Inhibition dominates sensory responses in the awake cortex. Nature 493:97–100. CrossRef Medline

Hofer SB, Mrsic-Flogel TD, Bonhoeffer T, Hübener M (2009) Experience leaves a lasting structural trace in cortical circuits. Nature 457:313–317. CrossRef Medline

Holtmaat A, Svoboda K (2009) Experience-dependent structural synaptic plasticity in the mammalian brain. Nat Rev Neurosci 10:647–658. CrossRef Medline

Jeanne JM, Sharpee TO, Gentner TQ (2013) Associative learning enhances population coding by inverting interneuronal correlation patterns. Neuron 78:352–363. CrossRef Medline

Joshua M, Adler A, Prut Y, Vaadia E, Wickens JR, Bergman H (2009) Synchronization of midbrain dopaminergic neurons is enhanced by rewarding events. Neuron 62:695–704. CrossRef Medline

Kerr JN, Greenberg D, Helmchen F (2005) Imaging input and output of neocortical networks in vivo. Proc Natl Acad Sci U S A 102:14063–14068. CrossRef Medline

Knott GW, Quairiaux C, Genoud C, Welker E (2002) Formation of dendritic spines with GABAergic synapses induced by whisker stimulation in adult mice. Neuron 34:265–273. CrossRef Medline

Ko H, Hofer SB, Pichler B, Buchanan KA, Sjöström PJ, Mrsic-Flogel TD (2011) Functional specificity of local synaptic connections in neocortical networks. Nature 473:87–91. CrossRef Medline

Kohn A, Smith MA (2005) Stimulus dependence of neuronal correlation in primary visual cortex of the macaque. J Neurosci 25:3661–3673. CrossRef Medline

Komiyama T, Sato TR, O'Connor DH, Zhang YX, Huber D, Hooks BM, Gabitto M, Svoboda K (2010) Learning-related fine-scale specificity imaged in motor cortex circuits of behaving mice. Nature 464:1182–1186. CrossRef Medline

Leuner B, Glasper ER, Gould E (2010) Parenting and plasticity. Trends Neurosci 33:465–473. CrossRef Medline

Levy RB, Reyes AD (2012) Spatial profile of excitatory and inhibitory synaptic connectivity in mouse primary auditory cortex. J Neurosci 32:5609–5619. CrossRef Medline

Liu RC, Schreiner CE (2007) Auditory cortical detection and discrimination correlates with communicative significance. PLoS Biol 5:e173. CrossRef Medline

Liu RC, Linden JF, Schreiner CE (2006) Improved cortical entrainment to infant communication calls in mothers compared with virgin mice. Eur J Neurosci 23:3087–3097. CrossRef Medline

Lytton WW, Sejnowski TJ (1991) Simulations of cortical pyramidal neurons synchronized by inhibitory interneurons. J Neurophysiol 66:1059–1079. Medline

Mitchell JF, Sundberg KA, Reynolds JH (2009) Spatial attention decorrelates intrinsic activity fluctuations in macaque area V4. Neuron 63:879–888. CrossRef Medline

Moore GP, Segundo JP, Perkel DH, Levitan H (1970) Statistical signs of synaptic interaction in neurons. Biophys J 10:876–900. CrossRef Medline

Morita K, Kalra R, Aihara K, Robinson HP (2008) Recurrent synaptic input and the timing of gamma-frequency-modulated firing of pyramidal cells during neocortical "UP" states. J Neurosci 28:1871–1881. CrossRef Medline

Moser MB, Trommald M, Andersen P (1994) An increase in dendritic spine density on hippocampal CA1 pyramidal cells following spatial learning in adult rats suggests the formation of new synapses. Proc Natl Acad Sci U S A 91:12673–12675. CrossRef Medline

Movshon JA, Albright TD, Stoner GR, Majaj NJ, Smith MA (2003) Cortical responses to visual motion in alert and anesthetized monkeys. Nat Neurosci 6:3; author reply 3–4. CrossRef Medline

Nauhaus I, Nielsen KJ, Callaway EM (2012) Nonlinearity of two-photon Ca^{2+} imaging yields distorted measurements of tuning for V1 neuronal populations. J Neurophysiol 107:923–936. CrossRef Medline

Noirot E (1972) Ultrasounds and maternal behavior in small rodents. Dev Psychobiol 5:371–387. CrossRef Medline

Ohiorhenuan IE, Mechler F, Purpura KP, Schmid AM, Hu Q, Victor JD (2010) Sparse coding and high-order correlations in fine-scale cortical networks. Nature 466:617–621. CrossRef Medline

Oviedo HV, Bureau I, Svoboda K, Zador AM (2010) The functional asymmetry of auditory cortex is reflected in the organization of local cortical circuits. Nat Neurosci 13:1413–1420. CrossRef Medline

Perin R, Berger TK, Markram H (2011) A synaptic organizing principle for cortical neuronal groups. Proc Natl Acad Sci U S A 108:5419–5424. CrossRef Medline

Recanzone GH, Schreiner CE, Merzenich MM (1993) Plasticity in the frequency representation of primary auditory cortex following discrimination training in adult owl monkeys. J Neurosci 13:87–103. Medline

Rennaker RL, Carey HL, Anderson SE, Sloan AM, Kilgard MP (2007) Anesthesia suppresses nonsynchronous responses to repetitive broadband stimuli. Neuroscience 145:357–369. CrossRef Medline

Rothschild G, Nelken I, Mizrahi A (2010) Functional organization and population dynamics in the mouse primary auditory cortex. Nat Neurosci 13:353–360. CrossRef Medline

Sakata S, Harris KD (2009) Laminar structure of spontaneous and sensory-evoked population activity in auditory cortex. Neuron 64:404–418. CrossRef Medline

Salinas E, Sejnowski TJ (2000) Impact of correlated synaptic input on output firing rate and variability in simple neuronal models. J Neurosci 20: 6193–6209. Medline

Sasaki T, Takahashi N, Matsuki N, Ikegaya Y (2008) Fast and accurate detection of action potentials from somatic calcium fluctuations. J Neurophysiol 100:1668–1676. CrossRef Medline

Sato TR, Gray NW, Mainen ZF, Svoboda K (2007) The functional microarchitecture of the mouse barrel cortex. PLoS Biol 5:e189. CrossRef Medline

Shadlen MN, Newsome WT (1998) The variable discharge of cortical neurons: implications for connectivity, computation, and information coding. J Neurosci 18:3870–3896. Medline

Shamir M, Sompolinsky H (2006) Implications of neuronal diversity on population coding. Neural Comput 18:1951–1986. CrossRef Medline

Sompolinsky H, Yoon H, Kang K, Shamir M (2001) Population coding in neuronal systems with correlated noise. Phys Rev E Stat Nonlin Soft Matter Phys 64:051904. CrossRef Medline

Song S, Sjöström PJ, Reigl M, Nelson S, Chklovskii DB (2005) Highly nonrandom features of synaptic connectivity in local cortical circuits. PLoS Biol 3:e68. CrossRef Medline

Stosiek C, Garaschuk O, Holthoff K, Konnerth A (2003) In vivo two-photon calcium imaging of neuronal networks. Proc Natl Acad Sci U S A 100: 7319–7324. CrossRef Medline

Thiele A, Herrero JL, Distler C, Hoffmann KP (2012) Contribution of cholinergic and GABAergic mechanisms to direction tuning, discriminability, response reliability, and neuronal rate correlations in macaque middle temporal area. J Neurosci 32:16602–16615. CrossRef Medline

Tian L, Hires SA, Mao T, Huber D, Chiappe ME, Chalasani SH, Petreanu L, Akerboom J, McKinney SA, Schreiter ER, Bargmann CI, Jayaraman V, Svoboda K, Looger LL (2009) Imaging neural activity in worms, flies and mice with improved GCaMP calcium indicators. Nat Methods 6:875–881. CrossRef Medline

Vaadia E, Haalman I, Abeles M, Bergman H, Prut Y, Slovin H, Aertsen A (1995) Dynamics of neuronal interactions in monkey cortex in relation to behavioural events. Nature 373:515–518. CrossRef Medline

Weinberger NM (2004) Specific long-term memory traces in primary auditory cortex. Nat Rev Neurosci 5:279–290. CrossRef Medline

Xu T, Yu X, Perlik AJ, Tobin WF, Zweig JA, Tennant K, Jones T, Zuo Y (2009) Rapid formation and selective stabilization of synapses for enduring motor memories. Nature 462:915–919. CrossRef Medline

Yaksi E, Friedrich RW (2006) Reconstruction of firing rate changes across neuronal populations by temporally deconvolved Ca^{2+} imaging. Nat Methods 3:377–383. CrossRef Medline

Yang G, Pan F, Gan WB (2009) Stably maintained dendritic spines are associated with lifelong memories. Nature 462:920–924. CrossRef Medline

Zohary E, Shadlen MN, Newsome WT (1994a) Correlated neuronal discharge rate and its implications for psychophysical performance. Nature 370:140–143. CrossRef Medline

Zohary E, Celebrini S, Britten KH, Newsome WT (1994b) Neuronal plasticity that underlies improvement in perceptual performance. Science 263:1289–1292. CrossRef Medline